DRO
Deakin University's Research Repository
DEAKIN UNIVERSITY AUSTRALIA Worldly

This is the published version:

Greene, George W., Olszewska, Anna, Osterberg, Monika, Zhu, Haijin and Horn, Roger 2013, A cartilage-inspired lubrication system, *Soft matter*, vol. 10, no. 2, pp. 374-382.

Available from Deakin Research Online:

http://hdl.handle.net/10536/DRO/DU:30058684

Reproduced with the kind permission of the copyright owner.

Copyright : 2013, RSC Publishing

dro.deakin.edu.au
Deakin University CRICOS Provider Code: 00113B

Soft Matter

PAPER

View Article Online
View Journal | View Issue

A cartilage-inspired lubrication system

Cite this: *Soft Matter*, 2014, **10**, 374

George W. Greene,*[a] Anna Olszewska,[b] Monika Osterberg,[b] Haijin Zhu[c] and Roger Horn[a]

Articular cartilage is an example of a highly efficacious water-based, natural lubrication system that is optimized to provide low friction and wear protection at both low and high loads and sliding velocities. One of the secrets of cartilage's superior tribology comes from a unique, multimodal lubrication strategy consisting of both a fluid pressurization mediated lubrication mechanism and a boundary lubrication mechanism supported by surface bound macromolecules. Using a reconstituted network of highly interconnected cellulose fibers and simple modification through the immobilization of polyelectrolytes, we have recreated many of the mechanical and chemical properties of cartilage and the cartilage lubrication system to produce a purely synthetic material system that exhibits some of the same lubrication mechanisms, time dependent friction response, and high wear resistance as natural cartilage tissue. Friction and wear studies demonstrate how the properties of the cellulose fiber network can be used to control and optimize the lubrication and wear resistance of the material surfaces and highlight what key features of cartilage should be duplicated in order to produce a cartilage-mimetic lubrication system.

Received 6th August 2013
Accepted 11th October 2013

DOI: 10.1039/c3sm52106k

www.rsc.org/softmatter

Published on 14 October 2013. Downloaded by Deakin University on 12/12/2013 00:34:10.

Introduction

Articular cartilage is an example of a highly efficacious, water-based natural tribological system that is optimized to provide low friction and wear protection at both low and high loads and sliding velocities, with the capability to resist serious damage over a typical lifespan (*i.e.* 75 years). Most attempts to create synthetic or artificial cartilage have focused on mimicking just one aspect of articular cartilage, for instance its mechanical properties[1] or the lubricating action of glycoproteins in joints.[2,3] These approaches generally ignore the fact that cartilage as a whole system has many aspects working synergistically to give rise to its superior tribological performance.[4–11]

At the heart of the cartilage lubrication system is a special kind of fluid pressurization mediated mechanism that is unique to biphasic materials—*i.e.* soft, porous materials whose pores are filled with interstitial fluid.[8,10,12] Though much debate still surrounds the specific details and mechanics of the process, experiments by Soltz and Athesian[12–14] have shown convincingly that the observed friction forces measured in articular cartilage are inversely correlated with the pressure in cartilage's interstitial fluid when sheared under a compressive load. In the fluid pressurization mediated lubrication model,[12] sometimes referred to as 'linear biphasic theory',[15] when two apposing porous materials are compressed, the interstitial fluid within the pore network becomes pressurized. The pressurized interstitial fluid supports the majority of the compressive load meaning that very little of the loading stress is actually carried by the solid phase (*i.e.* the collagen fibril network) leading to reduced friction forces and greater resistance to wear.[10,12]

One of the defining characteristics of the fluid pressurization lubrication mechanism is the different friction responses observed when the friction measurements are performed in both static and migrating contact position geometries. With the static contact geometry, a time dependent friction response is observed in which the friction coefficient is initially low but increases with time as the surfaces are sheared. This time dependent response has previously been shown to be controlled by the pressurization and subsequent dissipation of interstitial fluid pressure where the time required to achieve a constant equilibrium value in the friction coefficient, μ_{eq}, equals the time required for the interstitial fluid pressure to completely dissipate.[8,14] However, as Ateshian *et al.*[12] have shown, when the same experimental measurement is performed using a migrating contact position geometry, a time dependent friction response is no longer observed. Instead, the friction coefficients measured were found to remain more or less constant and roughly equal to the initially low values measured in the static position geometry. The reason for the different friction responses between the static and migrating contact position geometries is that the pressurized interstitial fluid supports the large majority of the loading stress (as much as 99% in cartilage[16]) resulting in very little stress (and thus friction) being borne by the solid pore network so long as the pressure in the

[a]*Institute of Frontier Materials, Deakin University, Burwood, Victoria, Australia 3125. E-mail: wren.greene@deakin.edu.au; Tel: +61 392468278*

[b]*School of Chemical Technology, Department of Forest Products Technology, Aalto University, Finland FI-00076*

[c]*Institute of Frontier Materials, Deakin University, Geelong, Victoria, Australia 3220*

This journal is © The Royal Society of Chemistry 2014

Published on 14 October 2013. Downloaded by Deakin University on 12/12/2013 00:34:10.

fluid remains high. Under a static contact position, the fluid pressure, though initially high, is able to slowly dissipate leading to more and more of the loading stress being transferred to the solid phase and, thus, an increase in the friction forces. Under a migrating contact position, the pressure in the fluid phase is never given sufficient time to dissipate before the area of the applied stress is moved and so the fraction of the loading stress supported by the solid phase (and the resulting friction forces) always remains low.[12,16]

However, merely replicating (or approximating) the structure and properties of cartilage's collagen fibril network is not sufficient to fully reproduce the fluid pressurization mediated lubrication mechanism. In cartilage, numerous highly charged macromolecules, collectively known as proteoglycans, are entangled within the collagen fibril network and are effectively immobilized.[3,17–19] The presence of a high density of immobile charge centers on the proteoglycan complexes gives the cartilage what is referred to as a fixed charge density†; essentially the number of immobile charges normalized by the volume.[20] Because the charges on the proteoglycans are overwhelmingly negative, they attract a larger number of cations into the tissue than anions creating a slight charge imbalance and an osmotic pressure gradient.[19,20] In addition, the charged macromolecular proteoglycans in cartilage give rise to large electro-steric (repulsive) forces that oppose the consolidation of the porous cartilage when under compression. These electro-steric forces together with the large osmotic pressure give cartilage a higher effective 'stiffness' in compression, slowing the rate of fluid loss and so prolonging the fluid load support (*i.e.* time dependent friction response).[20]

Fluid pressure mediated lubrication is effective, but it is unable on its own to provide the required lubrication and wear protection at all times, particularly when cartilage is subjected to large and prolonged compressive loads. For those times, nature has evolved biological boundary lubricants, most notably the proteoglycan lubricin[21–24] and the polysaccharide hyaluronic acid.[7,9,25] These biological boundary lubricant molecules are able to reduce the friction forces and protect against wear at the sites where apposing cartilage surfaces may come into solid–solid contact (*i.e.* the points where the stresses carried by the collagen fibril network are highest). Together, fluid pressurization and boundary lubrication function cooperatively and synergistically so that the optimal lubrication and protection of cartilage surfaces can be provided under a wide range of loading and shearing conditions and histories.[7,11]

Here we describe a synthetic tribological system that successfully mimics two of cartilage's primary lubrication processes, fluid pressurization and boundary lubrication. A reconstituted cellulose fiber network (CFN) is used to mimic the structural, mechanical, and fluid transport properties of the collagen fibril network of cartilage tissues. We modify the surfaces of the CFN with adsorbed molecules of the negatively charged biopolyelectrolyte carboxymethylcellulose (CMC), which mimic the electro-steric contributions of the proteoglycan macromolecular complexes in cartilage and allow for the deformation and fluid transport response (*i.e.* fluid pressurization and dissipation) of the CFN to be controlled under a compressive load. Finally, we introduce a graft copolymer consisting of a long CMC backbone with much shorter chains of polyethylene glycol (PEG) to the lubricant fluid which functions as a boundary lubricant to provide additional lubrication and wear protection at sites where the shearing surfaces may come into physical contact.

† The term 'fixed charge density' in the cartilage research community is used to refer to the number of charge carrying species per unit volume that is not displaced within or expelled from the cartilage when it is deformed. This 'fixed charge density,' however, can change if the pH and/or ionic strength of the interstitial fluid changes.

Methods and materials

Preparation of the cellulose fiber network

A network of interconnected cellulose fibers having a morphology similar to the superficial zone of cartilage's collagen fibril network (in terms of porosity and pore size distribution) was prepared by the recrystallization of cellulose from solution using a method previously developed by S. Deguchi, *et al.*[26] First, a 7% wt cellulose solution was prepared by adding microcrystalline cellulose powder (Sigma-Aldrich, St. Louis, MO) to a saturated aqueous solution of calcium thiocyanate (Sigma-Aldrich, St. Louis, MO). The cellulose powder was stirred in the calcium thiocyanate solution at room temperature for one hour to homogenize the suspension and allow time for the thiocyanate to begin reacting with the cellulose chains. After this initial incubation period, the cellulose suspension was transferred to a sealed glass syringe and heated to 120 °C in an autoclave and held at this temperature for 15 minutes to dissolve the cellulose. At this point, the cellulose solution was removed from the autoclave and the hot solution was immediately injected into a stainless steel cavity mold and allowed to cool to room temperature. For the CFN 'disks,' a mold with a 2 mm deep, 8 cm diameter cylindrical cavity was used while for the CFN 'pins,' a 1 cm diameter truncated spherical cavity with a 2 cm radius of curvature was used. The cooled cellulose solution (now a translucent, thick, non-flowing gel) was then immersed while still in the cavity mold in a 250 mL bath of methanol in order to leach out the calcium thiocyanate and cause the cellulose to crystallize into an interconnected network of fibers (see Fig. 1). The methanol in the bath was exchanged approximately every hour until the cellulose gel completely changed from translucent to an opaque white gel which also corresponded roughly with the point that the gel naturally released itself from the cavity; typically 2–3 hours for the larger disks and 1–2 hours for the smaller pins. The demolded, opaque CFN gels were then placed in a DI water-filled dialysis tube which was submerged in a 5 L bath of DI water for at least 24 hours to remove any residual calcium thiocyanate still remaining in the gels.

Chemical modification of the cellulose fiber networks

In order to control the deformation rate and thus the duration of the fluid pressurization lubrication mechanism, the molded

Published on 14 October 2013. Downloaded by Deakin University on 12/12/2013 00:34:10.

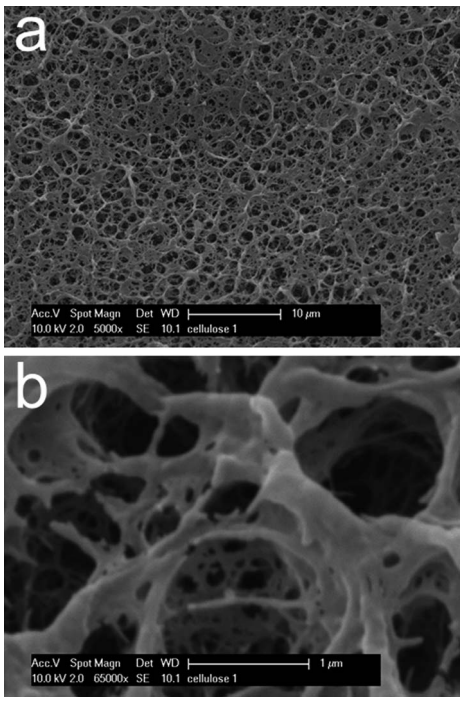

Fig. 1 SEM micrographs showing the CFN microstructure at (a) low and (b) high magnification. Samples were prepared by freeze drying in order to preserve the 'swollen' structure of the CNF and were coated with a roughly 30 nm thick conductive gold film for imaging.

CFN samples were modified by the physical adsorption of carboxymethylcellulose (CMC; Sigma-Aldrich, St. Louis, MO) polymer chains having an average molecular weight of 90 kDa. This modification was carried out by submerging the CFN samples into solution of CMC of different concentrations (from 0–2.5% wt) in phosphate buffer saline for 24 hours to allow sufficient time for the CMC to completely diffuse into the pore structure and equilibrium to be established. After the modification with adsorbed CMC, the modified CFN samples were soaked in excess PBS for approximately 1 hour in order to allow most of the unbound CMC molecules to diffuse out of the CFN.

Solid state NMR measurements

Solid state NMR was used to qualitatively assess (*i.e.* relative to one another) the amount of CMC that was effectively immobilized to the internal and external surfaces of the CFN during modification with solutions of different CMC concentration. Unmodified and CMC-modified CFN samples were prepared for the NMR measurements by first drying the samples in a vacuum oven at 50 °C and a pressure of −100 kPa for 48 hours to remove the water from the samples. The dried samples were then ground to a fine powder using a mortar and pestle before packing into the NMR rotor for measurements. All the solid state NMR experiments were performed on a Bruker Avance III wide bore spectrometer operating at 1 h Larmor frequency of 300.13 MHz. A standard 4 mm HFX double resonance magic angle spinning (MAS) probe head was used for all the measurements. The MAS frequency of 10 kHz and 90° pulse duration of 4 μs were used for the CP-MAS experiments. Typically 16k transients with recycle delay of 5 s were collected for each spectrum in order to get sufficient signal to noise ratio. All the measurements were performed at ambient temperature (298 K).

Carboxymethylcellulose-poly(ethylene glycol) graft copolymer lubricant solution

Some experiments in this report were run using 1% wt solutions of a carboxymethylcellulose–polyethylene glycol (CMC–PEG) graft-copolymer, which functions as a boundary lubricant, dissolved in phosphate buffered saline (PBS; pH 7.4). This polymer was synthesized following a procedure described in ref. 27. The CMC–PEG consists of CMC backbone having an average M_w of 250 kDa which is decorated by numerous and much smaller PEG side-chains having an average M_w of 2 kDa giving the copolymer a 'bottle-brush' morphology. Approximately one in every 8.5 carboxyl monomer units has been modified with a grafted PEG chain leading to an average distance between grafted PEG chains of 6 nm. This polymer has previously been shown to provide effective boundary lubrication of nanofiber cellulose films, reducing the measured friction coefficient by as much as 88%.[28]

Friction measurements

Friction measurements were performed using a Nanovea pin-on-disk tribometer (Nanovea, Irvine, CA). In this report, two different experimental configurations were used: a 2 cm radius of curvature CFN 'pin' against a 316 series stainless steel 'disk' (referred to in this report as the 'CFN pin geometry' which gives a static contact position) and a 6 mm diameter 100 CR6 High Chrome Steel 'pin' against a CFN 'disk' (referred to as the 'CFN disk geometry' which gives a migrating contact position). Friction measurements were performed over a range of dead weight loads from 1–4 N and at a relatively low shear rate of 50 mm min^{-1} (unless otherwise noted in the text) to avoid the possibility of entering a hydrodynamic lubrication regime which could complicate the analysis of the CFN gel's friction properties. The relevant experimental conditions under which specific friction measurements were collected are described in the figure legends for the corresponding data sets. Unfortunately, at the low loads and shear rate at which these measurements had to be run, very slight irregularities in the 'flatness' of the tribometer's rotation stage led to small periodic oscillations in the measured friction force on the order of ±0.15 N being observed (see Fig. 6 below). Since these oscillations were completely correlated with the rotation angle of the rotation stage and did not change their periodicity when different loads were applied‡, it was concluded that they were the result of small irregularities in the rotational stage (*i.e.* deviations from true flatness). For this reason, the friction data presented in Fig. 2 and 4 has been 'smoothed' using an adjacent-averaging function. The averaging 'window' was set to the minimum number of data points

‡ A change in the friction force oscillation frequency would be expected if, for instance, the oscillations in the measured forces were caused by a tribological phenomenon such as stick-slip sliding.

 This journal is © The Royal Society of Chemistry 2014

Published on 14 October 2013. Downloaded by Deakin University on 12/12/2013 00:34:10.

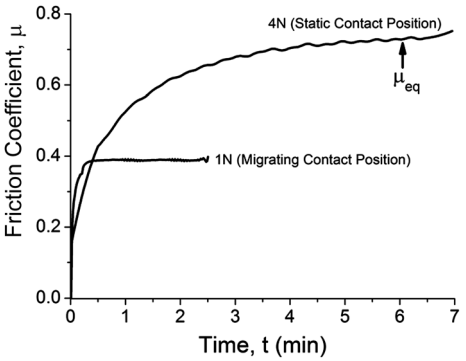

Fig. 2 The friction responses of the unmodified CFN measured in both the static contact position geometry, under a constant load of 4 N (minimum pressure ≈ 0.32 MPa), and migrating contact position geometry, under a constant load of 1 N (approximate pressure at center of contact ≈ 0.30 MPa) the equilibrium friction coefficient, μ_{eq}, corresponds to the region of the time dependent friction response curve (static contact position) where the value of μ settles into a constant value and no longer changes with time.

necessary to remove the majority of the oscillation noise. The adjacent-averaging was effective at removing the noise from the data without altering the overall shape of the friction curves. The main drawback of this method; however is the loss of information around the first and last 10–20 seconds of time dependent friction coefficient, μ, and leads to a small error in the value of μ near $t = 0$ where the value of μ changes most rapidly and in some cases a false upturn in apparent friction at the end of a run. The smoothing procedure used to remove the systemic oscillations in the measured μ, however, did not significantly alter the general shape or trends of the dynamic, time-dependent friction response presented in this report.

Mechanical testing

The mechanical creep response of the CMC modified and unmodified CFN samples were performed using a TA instruments Q800 Dynamic Mechanical Analyser. The tests were performed on the molded CFN 'pin' samples described in the 'Preparation of the cellulose fiber network' subsection of the Methods and materials. The CFN pins were compressed between two parallel steel plates under an instantaneously applied loading force of 3 N and the distance between the two plates (*i.e.* the compressive deformation of the CFN) was monitored over time. All tests were performed in air and at ambient temperature.

Wear characterization

Wear of the CFN materials was imaged using white light interferometry in a Bruker GT-K1 optical profilometer at 10× magnification. The images of the surface topography were analyzed using the bundled Vision 64 software package.

Results and discussion

In this report, a CFN which shares many of the same structural and physical properties of cartilage's collage fibril network was used as the porous platform. SEM images showing the CFN's pore microstructure are provided in Fig. 1a and b. Visual inspection of the SEM micrographs in Fig. 1a and b shows that the porosity of the cellulose gel consists of a range of pore sizes varying roughly from 1–2 μm to approximately 100 nm. Gravimetric analysis comparing the differences between the wet and dry masses showed that the mass fraction of water in the CFN to be approximately 0.89.

Cellulose shares much in common with the type II collagen. Like type II collagen, cellulose naturally crystallizes into fibers which bend easily under a compressive or bending stress yet can still support very large tensile stresses with very little elongation (it is this property that makes cellulose fibers such a useful material for ropes). Like cartilage, this allows fluid swollen networks of cellulose fibers to deform comparatively easily along the loading axis while at the same time resisting the orthogonal expansion of the network (*i.e.* a very low Poisson's ratio). The tensile stresses in the cellulose fiber network resist the lateral expansion of network under a compressive stress that would result in a volume conserving deformation response and, as a result, is able to maximize the pressure retained in the interstitial fluid. The Poisson ratio of the unmodified CFN material was found to be 0.11 ± 0.02. This value of the Poisson's ratio is less than the range of values typically reported for articular cartilage tissues (*e.g.* ~0.3–0.18).[29,30] The measurement of the Poisson ratio was performed by compressing a 6 mm diameter disk to 50% of its uncompressed thickness between parallel plates and measuring the change in the disk's diameter. Given the similarities in the physical properties and microstructures of the cellulose fiber network and cartilage's collagen fibril network, the interstitial fluid in the CFN is expected to develop, initially, a very high pressure upon loading (and thus a fluid pressurization lubrication response) similar to what is seen in articular cartilage when loaded and sheared.

The fluid pressurization lubrication mechanism of cartilage tissues is well known and has been the subject of significant experimental and theoretical research.[10,12,14,20] In order to verify whether or not the CFN gives rise to a fluid pressurization lubrication mechanism, it is necessary to test the friction response of the material in both a static and migrating contact position geometry under identical loading and shearing conditions (Fig. 2). Fig. 2 shows the friction responses of an unmodified cellulose gel pin against a steel disk (*i.e.* static contact position geometry) and a steel pin against a cellulose gel disk (*i.e.* migrating contact geometry) at a shear rate of 50 mm min^{-1} in PBS. The dead weight load was 4 N for the static contact position geometry (minimum loading pressure = 0.32 MPa) and 1 N for the migrating contact position geometry approximate loading pressure at the center of contact = 0.30 MPa; estimated using the Hertzian contact model for an elastic spherical indenter against a flat surface.[31] In the static contact position, a time dependent friction response similar to real articular cartilage tissues was observed; however, the time required to reach μ_{eq} was much shorter than is typically observed in real cartilage under similar conditions.[7,10,12] While the CFN took roughly 5 min to reach a constant equilibrium friction coefficient of $\mu_{eq} = 0.72$, in real cartilage the time to

Published on 14 October 2013. Downloaded by Deakin University on 12/12/2013 00:34:10.

reach μ_{eq} (=0.15–0.25 under similar loading and shearing conditions) is typically on the order of 30–45 min.[7,12] In contrast, no time dependent friction response is observed in the migrating contact position geometry where the friction coefficient rapidly reaches a constant equilibrium of $\mu_{eq} = 0.38$ in a few seconds and remains much lower than the equilibrium friction coefficient measured in the static contact geometry. This difference in the static and migrating contact position friction responses is qualitatively the same as cartilage and provides compelling evidence of the presence of a fluid pressurization lubrication mechanism at work in the unmodified CFN. However, the duration of the time dependent response and the ultimate value of μ_{eq} needs to be considerably lengthened and reduced respectively before truly capturing the frictional properties of real cartilage tissue.

In order to fully reproduce the time dependent friction response of cartilage in the cellulose fiber networks, it is necessary to replicate in the cellulose system two critical aspects of the cartilage lubrication system: (1) the immobilization of a highly charged polyelectrolyte within the porous network to create a fixed charge density and electro-steric repulsive forces required to control the deformation and swelling responses and, (2) a boundary lubricating molecule (similar to lubricin protein) to reduce the friction forces and wear at points of solid–solid contact.

The cellulose fiber networks were given a fixed charge density by modifying the surfaces of the CFN with physically adsorbed layers of CMC from PBS solutions with different concentrations between 0.75% wt to 2.5% wt (see Materials and methods). To provide the system with boundary lubrication, a carboxymethylcellulose–polyethylene graft copolymer (CMC–PEG; described in the Materials and methods section) was synthesized and added to the PBS lubricant fluid at a concentration of 1% wt. A schematic of the modified cellulose lubrication system is shown in Fig. 3a.

While quantifying the total amount of CMC immobilized at the surfaces of the CFN is difficult due to the similarity in the molecular and chemical structure of CMC and cellulose, ^{13}C NMR spectroscopy enables the relative concentrations of immobilized CMC to be ascertained. Fig. 3b shows the ^{13}C NMR spectra collected for the various CMC modified CFNs while the integrated areas of the C=O peak (a unique functional group located only on molecules of CMC and located at a chemical shift of ~178 ppm) are provided in Table 1. The NMR spectra in Fig. 3b indicates clearly that the modification of the CFNs in the solutions of CMC leads to the adsorption and effective immobilization of CMC molecules and that the intensity of the C=O peak detected increases with the concentration of CMC in the solution. Integration of the C=O peak area (relative to the total area of the NMR signal) is given in Table 1 and provides a convenient means in which to compare, qualitatively, the relative amount of CMC immobilized within the different CFN samples. And since all the C=O groups in the CMC molecule are associated with the carboxylic acid functional groups which

Table 1 The integrated area of the C=O peak in the CP-MAS solid state NMR spectra (shown in Fig. 3b) collected for the CFN samples modified with PBS solutions having different concentrations of CMC. The integrated area provided is expressed as the integrated area of C=O peak relative to the total integrated area of the overall NMR signal

Sample	Integrated area of C=O peak
0% CMC	≈0
0.75% CMC	≈1/531
1.25% CMC	1/385
2.5% CMC	1/133

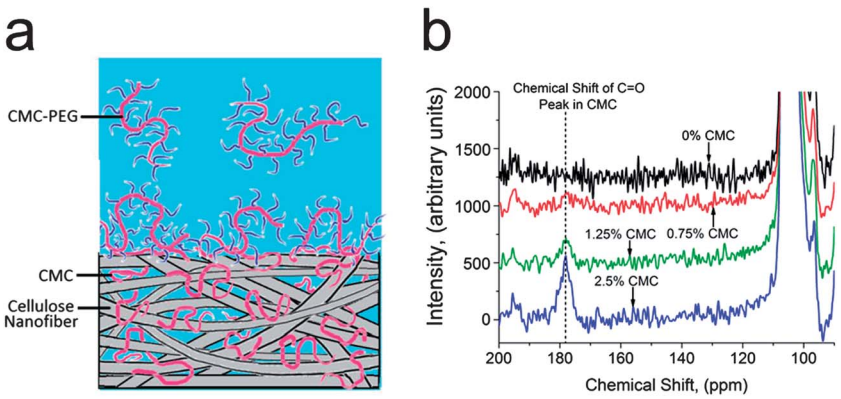

Fig. 3 (a) Schematic illustration of the modified CFN. The internal surfaces of the CFN are chemically modified by a physically adsorbed layer of CMC molecules to create a fixed charge density in the material and an osmotic pressure gradient (with the fluid reservoir) which, together with electrostatic and steric repulsive forces produced by the adsorbed CMC molecules, controls the deformation rate of the CFN under compression. In certain measurements, a CMC-peg graft copolymer is added to the lubricating fluid (PBS) which functions as a boundary lubricant that lowers friction forces and wear at points of physical contact between the CFN (shearing) surface and the surface of the stainless steel testing disk. (b) The cp-mas solid state NMR spectra collected for the CFN samples modified with PBS solutions having different concentrations of CMC. The peak at ~178 ppm corresponds to the chemical shift of the C=O groups in the CMC molecules which provides a means to qualitatively assess the relative amounts of CMC immobilized to the CFNs (*i.e.* the integrated peak area given in Table 1) after being modified with CMC solutions of increasing concentration.

This journal is © The Royal Society of Chemistry 2014

Published on 14 October 2013. Downloaded by Deakin University on 12/12/2013 00:34:10.

are the sole charge carrying species, the integrated area is also proportional to the fixed charge density in the modified CFNs (assuming that the dissociation constant of the CMC in each sample is the same). As seen in Table 1, the amount of CMC immobilized to (and the fixed charge density of) the CFN modified with the 2.5% wt solution of CMC is approximately 2.9 and 4.0 times higher than the CFNs modified with the 1.25% wt and 0.75% wt CMC solutions respectively.

The time dependent friction responses of the CMC modified cellulose fiber networks, shown in Fig. 4, were measured in a static contact position geometry under a 3 N static load and shear rate of 50 mm min^{-1}. Friction measurements were conducted on the CMC modified CFN using both pure PBS and a 1% wt solution (in PBS) of the CMC–PEG boundary lubricant. While the addition of the CMC–PEG to the PBS caused the viscosity of the fluid to increase modestly, this difference in viscosity will have no significant impact due to the very low shear rates used that keeps the system in a load controlled friction regime where hydrodynamic processes (*i.e.* fluid viscosity and shear rate) have no influence on the friction forces measured. First, looking at the friction responses of the CMC modified CFN measured in pure PBS (solid lines), it is clear that as the level of CMC immobilized to the CFN (*i.e.* the fixed charge density) increases, the time required to reach a constant equilibrium friction coefficient μ_{eq} increases from roughly 4 minutes (for 0% CMC) to approximately 35 minutes (for 2.5% CMC) and the value of μ_{eq} decreases modestly from $\mu_{eq} \approx 0.6$ to $\mu_{eq} \approx 0.45$. Although the friction response time of 35 minutes observed in the 2.5% CMC sample is approximately equal to that observed in real cartilage tissues under similar loading and shearing conditions,[7,42] it is a bit misleading for the following reason. While increasing the amount of CMC adsorbed to the CNF surfaces increased the observed time to reach μ_{eq}, it also led to a significant amount of visible wear in all the CMC modified CFN samples which could possibly be caused by some adhesive interactions between the adsorbed CMC layer and the stainless steel disk. The time dependent friction response observed thus reflects both the changing friction forces due to the fluid pressurization lubrication mechanism and the wear process which changes the structure and topography of the CFN surface.

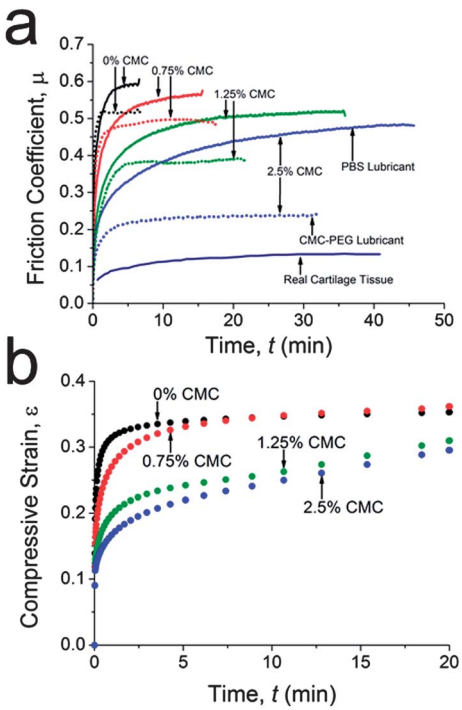

Fig. 4 Plot of the time dependent friction responses (a) and time dependent deformation response (b) of different CFN modified with increasing amounts of physically adsorbed CMC. The friction responses shown in (a) were measured using both PBS (solid lines) and 1% wt CMC-PEG in PBS (dotted lines) as the lubricant fluid. All measurements were conducted in the static contact position geometry under a constant load force of 3 N (minimum pressure ≈ 0.24 MPa) and at a shear rate of 50 mm min^{-1}. For comparison, the time dependent friction response of real cartilage measured in a surface forces apparatus under similar loading pressures and previously reported in ref. 4 has also been plotted. The mechanical responses shown in (b) were all measured under a static, instantaneously applied load of 3 N.

Evidence of wear appeared in the form of visible 'wear tracks' in the sheared regions of the CMC modified CFN surfaces tested using PBS as the lubricant fluid shown in Fig. 4a. In addition, a significant amount of micron sized 'wear debris' also was visible in the lubricant fluid when viewed using optical microscopy. A more detailed characterization of the changes in the surface topography due to wear in a 2.5% CMC modified CFN pin was made using an optical profilometer. As seen in Fig. 5, shearing the CMC modified CFN is PBS without the CMC–PEG lubricant present resulted in a change in the surface from initially relatively smooth (Fig. 5 a and a′) to being significantly rougher (Fig. 5b and b′). This roughening of the surface coincided with the appearance of relatively large parallel channels, microns wide and deep, oriented along the shearing axis. In contrast, the addition of the CMC–PEG boundary lubricant to the PBS lubricant fluid eliminated the vast majority of wear in the CFN surface (Fig. 5c and c′). Although numerous parallel groves oriented along the shearing axis do become visible in the profilometry data, these groves are significantly smaller and shallower than those seen in Fig. 5b and b′. Visual inspection of the lubricant fluid using optical microscopy also did not reveal the presence of any wear debris.

Because of the adhesion and significant wear occurring at the CMC modified CNF surfaces in the pure PBS lubricant, the duration of the time dependent friction response does not accurately reflect the friction response attributed solely to the action of fluid pressurization. However, the addition of the CMC–PEG boundary lubricant to the PBS eliminated the adhesion and significantly reduced the wear in the system, allowing the true friction response of the CMC modified CFN due to the fluid pressurization lubrication mechanism to be seen unobscured. As is seen in Fig. 4a, increasing the amount of CMC immobilized in the CFN (*i.e.* the fixed charge density) still leads to a significant prolongation of the time dependent friction response in the samples after the CMC–PEG boundary lubricant was added to the PBS fluid. This increases incrementally from roughly 2 minutes to reach μ_{eq} in the 0% CMC sample to roughly 12 min in the 2.5% CMC sample.

Published on 14 October 2013. Downloaded by Deakin University on 12/12/2013 00:34:10.

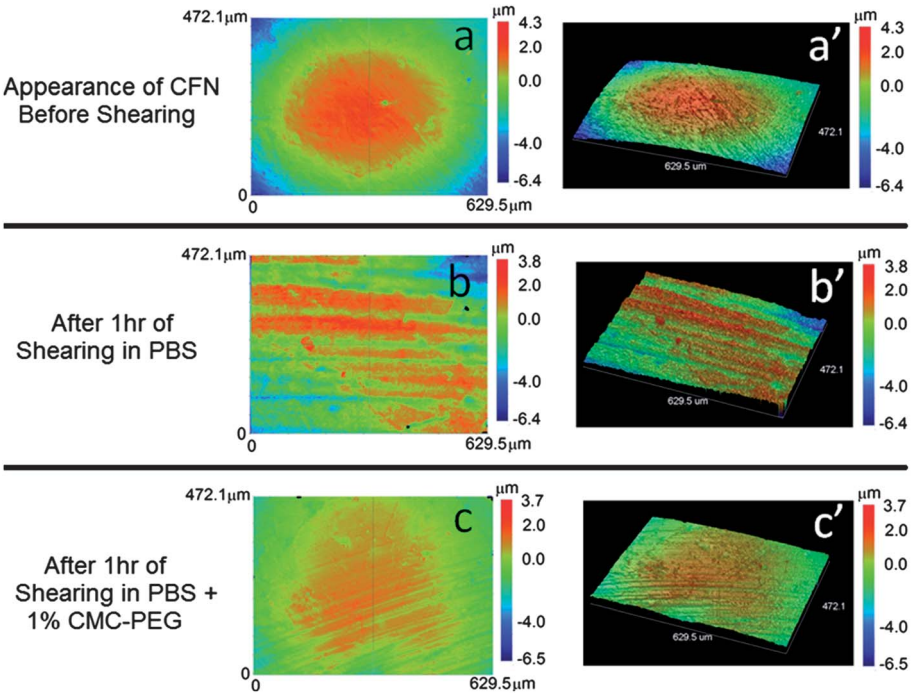

Fig. 5 Optical profilometry images showing the 2d (a–c) and 3d (a′–c′) surface topography of CFN pins modified with a 2.5% CMC solution measured before shearing (a and a′), after 1 h of shearing in PBS lubricant (b and b′), and after 1 h of shearing in PBS containing 1% wt CMC–PEG boundary lubricant. Shearing was performed at a shear rate of 50 mm min^{-1} against a stainless steel disk under a constant load of 3 N.

Measurement of the mechanical creep response of the modified and unmodified CFN materials under a constant load force of 3 N (see Fig. 4b) shows that increasing the amount of CMC bound to the CFN also leads to a significant prolongment of the deformation time and slowing of the observed deformation rate. Comparing the mechanical responses of the various CMC modified and unmodified CFN samples with the observed friction responses (with the CMC–PEG boundary lubricant) indicates that the observed time dependent change in the friction coefficient is strongly correlated with the mechanical deformation of the material (*i.e.* the dissipation of fluid pressure *via* flow). Such a strong correlation between the mechanical and friction response is a central feature of the fluid pressurization lubrication mechanism and indicates that as the fixed charge density (amount of immobilized CMC) in the CFN increases the material becomes effectively stiffer and better able to retain interstitial water and more slowly dissipate fluid pressure.

In addition to increasing the duration of the fluid pressurization lubrication mechanism, the addition of the CMC–PEG boundary lubricant also led to a significant decrease in the overall friction coefficient (forces) over the duration of the time dependent friction response and particularly the value of μ_{eq} for the all the tested samples. The decrease in μ_{eq} was most significant at higher CMC concentrations. This correlation between the reduction in friction coefficient and the amount of CMC adsorption indicates that the ability of the CMC–PEG to provide boundary lubrication (at least in this system) results largely from the formation of entanglements between the CMC–PEG and the adsorbed CMC layers rather than through direct physical bond formation between the cellulose and the CMC backbone of the CMC–PEG molecule. In the absence of CMC the reduction in μ_{eq} is considerably less.

For comparison, the time dependent friction response of real cartilage measured in a surface forces apparatus under similar loading pressures and previously reported in ref. 7 has also been plotted in Fig. 4. While the surface forces apparatus measurements were conducted using PBS as the lubricant fluid, the surfaces of the cartilage used in this measurement still retained a layer of physically adsorbed lubricin protein and mechanically immobilized, partially entangled hyaluronic acid which function as boundary lubricants similar to the CMC–PEG. We were able to reproduce a time dependent friction response in the CFN modified with a 2.5% wt CMC solution in the CMC–PEG lubricant fluid that was roughly 1/3 the duration of real cartilage tissue and achieve an equilibrium friction coefficient that was twice as large as the real cartilage (but still within the range of values that have been reported for cartilage in other research reports[7,10,12]).

Although a time dependent friction response in a static contact position geometry is one of the defining characteristics of the fluid pressurization lubrication mechanism, this type of lubrication is designed to function and indeed is most effective in systems where the contact position migrates. In real articular joints, where apposing surfaces move across one another *via* a combination of rolling and sliding that insures that regions of surfaces in actual contact constantly change, the effective friction coefficient is typically found to be between $\mu = 0.04$–0.005 (depending upon the loading and shearing velocities used in the measurement).[32] If the CMC modified CFN material is truly mimicking the fluid pressurization lubrication mechanism of

 This journal is © The Royal Society of Chemistry 2014

Published on 14 October 2013. Downloaded by Deakin University on 12/12/2013 00:34:10.

cartilage, then it too should be expected to exhibit a very low effective friction coefficient in a migrating contact position geometry.

Fig. 6 shows the friction response in a migrating contact position geometry of a CFN disk (against a stainless steel pin) that was modified by immersion in a 2.5% wt solution of CMC with a 1% wt solution of CMC–PEG boundary lubricant in PBS under a constant load of 1 N (estimated peak loading stress = 0.30 MPa). As is seen in Fig. 6, the observed friction coefficient rises quickly and settles into a stable equilibrium value in just a few tens of seconds as opposed to tens of minutes observed in the static contact position geometry (see Fig. 4) under similar loading pressures. In addition, in the migrating contact position geometry, the stable value of the friction coefficient was also found to be strongly dependent upon the shearing velocity, decreasing from a relatively high value of $\mu \approx 0.18$ to a much lower value of $\mu \approx 0.08$ when the shear velocity was increased from 50 to 300 mm min^{-1} (which is still much too slow for hydrodynamic lubrication processes to be significant). A shear velocity dependence is an expected consequence of the fluid pressurization lubrication mechanism.[12] Because the reduction in the effective friction force of the CFN is proportional to the interstitial fluid pressure, as the shear velocity (*i.e.* the contact position migration rate) increases the amount of time that a position of the CFN surface is subjected to the compressive load decreases. Consequently, the reduced loading time before the contact position migrates to a new, previously uncompressed position also decreases the amount of time that the fluid pressure under the loaded position is able to dissipate *via* flow. Consequently, the magnitude of the fluid pressure and the fraction of the loading stress carried by the fluid phase remains higher as the migration/shearing speed becomes faster resulting in a lower realized friction force. Even at a relatively slow shearing velocity of 300 mm min^{-1}, a very low friction coefficient of $\mu \approx 0.08$ is measured. However, despite being quite low, the friction coefficient of the modified CFN is still higher than the ultra-low values reported for articular cartilages (*e.g.* $\mu \approx 0.04$–0.005),[32] and most likely reflects, first, the superior ability of cartilage to retain and more slowly dissipate the interstitial fluid pressure under compressive loading compared to the modified CFN (as seen in cartilage's much slower time dependent friction response in Fig. 4) and, second, that lubricin protein and hyaluronic acid bound to cartilage's surfaces most likely provide more effective boundary lubrication compared to the CMC–PEG polymer.

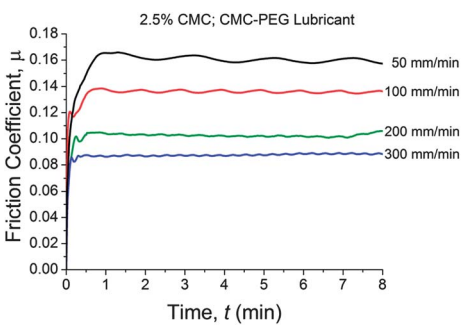

Fig. 6 Effect of shearing velocity on the friction response of a CFN disk modified with a 2.5% CMC solution against a stainless steel 'pin' (*i.e.* in a migrating contact position geometry) using a 1% wt CMC-PEG in PBS lubricant solution. All the measurements were performed using a static load of 1 N (approximate pressure at the center of contact ≈ 0.3 MPa).

Conclusions

We demonstrate that the complex, multi-modal lubrication system of cartilage that is central to its superior abilities to resist wear and damage can be partially mimicked (and controlled) in a synthetic system so long as three key features of the articular cartilage system are duplicated:

(1) At the core of the system, there needs to be a solid deformable network consisting of highly interconnected, submicron sized pores. The network must have a low permeability so that the flow of interstitial fluid is inhibited which allows the fluid to develop a very high pressure when subjected to a compressive load and to retain a high fluid pressure over an extended period of time by greatly restricting the flow of interstitial fluid within the network. The pressurized interstitial fluid supports the majority of the compressive load and the gradual dissipation of fluid pressure dampens impact shocks (rapid changes in the load). Gradients in the fluid pressure direct the flow of fluid within the porous platform critical to the fluid pressurization lubrication mechanism.

(2) Within the solid porous network, there needs to be a high concentration of immobilized, highly charged macromolecules. These highly charged macromolecules give rise to electro-steric repulsive forces that resist the consolidation of the network in compression and thus retard the rate of deformation (*i.e.* the dissipation of the fluid pressure). In addition, these large, immobilized charged molecules provide the solid network with a fixed charge density (*i.e.* a concentration of immobile charge centers) that gives rise to a large osmotic pressure gradient in the compressed network that enhances its effective stiffness and retention of interstitial fluid pressure. By varying the concentration of bound CMC in the CFN, it is possible to control the deformation/fluid pressure dissipation rate.

(3) A suitable boundary lubricant molecule capable of binding strongly to the surface must be present. Boundary lubrication is necessary to prevent the shearing surfaces from coming into solid–solid contact when shear rates are too low and/or loading intervals too long for the fluid pressurization lubrication mechanism to provide effective protection against wear by supporting the majority of the compressive loading stress.

We have incorporated these three key design features into a single, purely synthetic material to create a cartilage mimetic tribological system that combines the ability to reduce friction forces through the pressurization of interstitial fluid with the action of a boundary lubricating molecule that further reduces the friction forces where solid–solid contacts between surfaces may form. Together, the action of the fluid pressurization and boundary lubrication mechanisms work synergistically to allow the mimetic tribological system to protect itself from wear and

Published on 14 October 2013. Downloaded by Deakin University on 12/12/2013 00:34:10.

damage *via* the same lubrication processes utilized by articular cartilage. The cellulose based system described in this report is not yet mechanically tough nor robust enough for most practical applications. However, the principles demonstrated in this cartilage mimetic lubrication system could, in the future, be applied to other porous material platforms having better mechanical properties. With the right materials and careful design, there is a high possibility that this system, or one similar to it in design, can be duplicated using biocompatible and implantable materials; for instance, using hydrogels, electrospun nanofibers, or composite structures formed from polyvinyl alcohol or reconstituted silk materials in place of the current cellulose porous platform. Though these experiments are a first step, they suggest that with better optimization of such material properties such as the porous network structure, porosity, pore size distribution, fluid permeability, fixed charge density, and boundary lubrication, a synthetic material system that is functionally equal or even superior to cartilage tissues may be possible.

Acknowledgements

This work was partially funded by a Discovery Early Career Research Award (DE130101458) from the Australian Research Council. Dr George W. Greene would like to thank the Australian Research Council for their support.

Notes and references

1 M. I. Baker, S. P. Walsh, Z. Schwartz and B. D. Boyan, *J. Biomed. Mater. Res., Part B*, 2012, **100**, 1451–1457.
2 M. Chen, W. H. Briscoe, S. P. Armes and J. Klein, *Science*, 2009, **323**, 1698–1701.
3 A. Dedinaite, *Soft Matter*, 2012, **8**, 273–284.
4 G. W. Greene, B. Zappone, X. Banquy, D. W. Lee, O. Soderman, D. Topgaard and J. N. Israelachvili, *Soft Matter*, 2012, **8**, 9906–9914.
5 G. W. Greene, B. Zappone, O. Soderman, D. Topgaard, G. Rata, H. B. Zeng and J. N. Israelachvili, *Biomaterials*, 2010, **31**, 3117–3128.
6 G. W. Greene, B. Zappone, B. Zhao, O. Soderman, D. Topgaard, G. Rata and J. N. Israelachvili, *Biomaterials*, 2008, **29**, 4455–4462.
7 G. W. Greene, X. Banquy, D. W. Lee, D. D. Lowrey, J. Yu and J. N. Israelachvili, *Proc. Natl. Acad. Sci. U. S. A.*, 2011, **108**, 5255–5259.
8 G. A. Ateshian, H. Q. Wang and W. M. Lai, *J. Tribol.*, 1998, **120**, 241–248.
9 J. Yu, X. Banquy, G. W. Greene, D. D. Lowrey and J. N. Israelachvili, *Langmuir*, **28**, 2244–2250.
10 C. W. McCutchen, *Wear*, 1962, **5**, 1–17.
11 T. Murakami, H. Higaki, Y. Sawae, N. Ohtsuki, S. Moriyama and Y. Nakanishi, *Proc. Inst. Mech. Eng., Part J*, 1998, **212**, 23–35.
12 G. A. Ateshian, *J. Biomech.*, 2009, **42**, 1163–1176.
13 M. Soltz and G. Ateshian, *Ann. Biomed. Eng.*, 2000, **28**, 150–159.
14 M. A. Soltz and G. A. Ateshian, *J. Biomech.*, 1998, **31**, 927–934.
15 V. C. Mow, S. C. Kuei, W. M. Lai and C. G. Armstrong, *J. Biomech. Eng.*, 1980, **102**, 73–84.
16 S. Park, R. Krishnan, S. B. Nicoll and G. A. Ateshian, *J. Biomech.*, 2003, **36**, 1785–1796.
17 S. R. Eisenberg and A. J. Grodzinsky, *J. Orthop. Res.*, 1985, **3**, 148–159.
18 J. Klein, *Proc. Inst. Mech. Eng., Part J*, 2006, **220**, 691–710.
19 A. Maroudas, *Nature*, 1976, **260**, 808–809.
20 W. M. Lai, J. S. Hou and V. C. Mow, *J. Biomech. Eng.*, 1991, **113**, 245–258.
21 J. M. Coles, L. Zhang, J. J. Blum, M. L. Warman, G. D. Jay, F. Guilak and S. Zauscher, *Arthritis Rheum.*, 2010, **62**, 1666–1674.
22 G. D. Jay, *Curr. Opin. Orthop.*, 2004, **15**, 355–359.
23 B. Zappone, G. W. Greene, E. Oroudjev, G. D. Jay and J. N. Israelachvili, *Langmuir*, 2007, **24**, 1495–1508.
24 B. Zappone, M. Ruths, G. W. Greene, G. D. Jay and J. N. Israelachvili, *Biophys. J.*, 2007, **92**, 1693–1708.
25 M. Benz, N. H. Chen and J. Israelachvili, *J. Biomed. Mater. Res., Part A*, 2004, **71**, 6–15.
26 S. Deguchi, M. Tsudome, Y. Shen, S. Konishi, K. Tsujii, S. Ito and K. Horikoshi, *Soft Matter*, 2007, **3**, 1170–1175.
27 J. Araki, M. Wada and S. Kuga, *Langmuir*, 2000, **17**, 21–27.
28 A. Olszewska, K. Junka, N. Nordgren, J. Laine, M. W. Rutland and M. Osterberg, *Soft Matter*, 2013, **9**, 7448–7457.
29 J. S. Jurvelin, M. D. Buschmann and E. B. Hunziker, *J. Biomech.*, 1997, **30**, 235–241.
30 P. Kiviranta, J. Rieppo, R. K. Korhonen, P. Julkunen, J. Töyräs and J. S. Jurvelin, *J. Orthop. Res.*, 2006, **24**, 690–699.
31 R. G. Horn, J. N. Israelachvili and F. Pribac, *J. Colloid Interface Sci.*, 1987, **115**, 480–492.
32 H. Forster and J. Fisher, *Proc. Inst. Mech. Eng., Part H*, 1996, **210**, 109–119.

 This journal is © The Royal Society of Chemistry 2014